

This is an Open Access document downloaded from ORCA, Cardiff University's institutional repository:<https://orca.cardiff.ac.uk/id/eprint/114438/>

This is the author's version of a work that was submitted to / accepted for publication.

Citation for final published version:

McLeod, R.W.J , Roberts, W.H., Perry, I.A., Richardson, B.E. and Culling, J.F. 2018. Scanning laser Doppler vibrometry of the cranium when stimulated by a B71 bone transducer. *Applied Acoustics* 142 , pp. 53-58. 10.1016/j.apacoust.2018.07.033 file

Publishers page: <http://dx.doi.org/10.1016/j.apacoust.2018.07.033>

Please note:

Changes made as a result of publishing processes such as copy-editing, formatting and page numbers may not be reflected in this version. For the definitive version of this publication, please refer to the published source. You are advised to consult the publisher's version if you wish to cite this paper.

This version is being made available in accordance with publisher policies. See <http://orca.cf.ac.uk/policies.html> for usage policies. Copyright and moral rights for publications made available in ORCA are retained by the copyright holders.



Scanning laser Doppler vibrometry of the cranium when stimulated by a B71 bone transducer

McLeod, R. W J¹, Roberts W. H², Perry I.A², Richardson, B.E², Culling, J. F¹.

1. School of Psychology, Cardiff University, Tower Building, Park Place, Cardiff, United Kingdom.
CF10 SAT.
2. School of Physics and Astronomy, Cardiff University, Queen's Building, The Parade, Cardiff,
United Kingdom. CF24 3AA.

Abstract

Scanning laser Doppler vibrometry (LDV) has been used extensively to investigate the movement of the middle and inner ear, but has never been used to measure vibrations from a bone transducer travelling over the skin, subcutaneous tissue and cranium in a live subject. Using three scanning laser Doppler vibrometers we measured the displacement of the cranium in 3D in a live subject when stimulated by a B71 bone transducer placed 55 mm posterior to the external auditory canal. Four pure tones (250 Hz, 500 Hz, 1000 Hz, 2000 Hz) were presented separately via the bone transducer. The displacement of the scalp was imaged in four different areas (ipsilateral to the bone transducer in the temporoparietal region, contralateral temporoparietal region, occipital region and vertex) and linked to the phase of stimulation. Measured scalp motion was consistent with expected displacement of the underlying cranium. Rigid-body motion was the dominant mode of vibration at 250 Hz. At 1000 Hz a mass-spring effect was seen. At 500 Hz there was a transition frequency between vibration as a rigid-body and as a mass-spring. Higher frequencies (2000Hz) showed that wave transmission was the primary vibrational mode of sound transmission over the cranium. These results broadly support previous research studies but open up potential areas of interest in the investigation of differing skull resonance frequencies.

1. Introduction

The routes by which bone-conducted sound travels to the inner ear have been extensively investigated and modelled in both dry skulls and cadavers heads [1–3]. The major routes by which bone conduction

signals reach the inner ear, as outlined by Tonndorf, are thought to be via (a) inertial excitation of the ossicular chain (b) air-borne sound generated by movement of the ear canal walls [4] (c) direct excitation of the cochlea [5–7] (d) pressure wave transmission via cerebrospinal fluid [8]. One or more of these modes of sound transmission can facilitate hearing in patients with bone-anchored hearing aids (BAHAs). Bone-conducted sound can also be problematic in extremely loud environments such as an aircraft carrier flight deck or an MRI machine, where it bypasses conventional noise-protection equipment [9]. A greater understanding of how the skull vibrates at differing frequencies may allow improved design of hearing-protection devices (HPDs) as well as allowing optimisation of sound transfer to the inner ear via bone-anchored hearing aids (BAHAs).

Investigations of skull vibration have primarily focused on mechanical point impedance [1,10] and resonance frequencies [11,12]. These studies have employed the use of accelerometers and have found that there are no resonance frequencies in the skull below 500 Hz. They found large variations in the resonance frequencies of individuals that could not be explained by head width, length or circumference alone. Due to these findings the consensus is that differences in skull resonance frequency is likely due to geometrical differences within the skull structure [11].

Several studies have investigated resonances through their effect on lateralisation of bone-conducted sound in patients. Anti-resonance was identified at frequencies between 100-350 Hz by Håkansson et al. (1986). Anti-resonance reduces the vibration around the cochlea either directly via bone conduction or via the ossicular chain. This causes a marked drop in sound level at the cochlea. Stenfelt et al., (2000) also showed that anti-resonance was present at low frequencies at the cochlea ipsilateral to the bone transducer, causing the sound to be lateralised to the side contralateral to the point of stimulation. Håkansson et al., (1993) concluded that one of the major causes of lateralisation was the anti-resonance seen at different frequencies and that the resonance frequencies were likely to be less important.

Previous studies have been primarily focused around the vibrational characteristics of specific areas of the skull (usually close to the cochlea). These have primarily used dry bones or cadavers, although it is unknown how the vibrational characteristics of the skull may differ between a cadaver head and a live subject. It may be that the reduction in intracranial pressure present in a cadaver head could affect the surrounding skull's vibrational modes. Our focus was around how the skull as a whole vibrates in a live subject in 3D. The investigation employed a scanning laser Doppler vibrometer (LDV). This has been used extensively to investigate the physiology of the middle ear and tympanic membrane [8,13–16]. However, these investigations generally used temporal bones and only employed a single laser vibrometer. Use of a single vibrometer limited vibrational mode data collection to a single plane. In order to capture the vibrational modes of the skull in 3D we employed three scanning laser vibrometers focused on the same area simultaneously. This builds on the research by McKnight et al., 2013 [17] who also used three scanning laser vibrometers to investigate the vibratory response over a range of audible frequencies in dry skulls. Their research into the admittance frequency response and the 3D velocity of the skull surface found that the spherical shell model of skull motion best fitted their findings. This model proposes that the skull can be represented as a spherical shell which supports twisting and elongation parallel to the skull surface but is incompressible in the thickest direction.

The aims of this study were as follows:

1. Evaluate the possibility of using three vibrometers simultaneously in the investigation of bone-conducted sound through skin-surface vibration. This measurement technique has been used previously in live subjects [18] but not to investigate bone-conducted sound. Where the technique has been used to evaluate bone-conducted sound, dry skulls were employed [17]. Thus, it is unclear if the use of a living participant will be possible as there will be interference from head movement as well as limitations on the time taken for measurements.

2. Measure the skull vibration of the whole skull in 3D. This is possible since the system used links the stimulus with the phase of the displacement at any point. This allows several different areas of the skull to be imaged separately and then reconstructed and linked to the same point in the phase cycle.

2. Materials and Methods

2.1. Ethical Approval

The following experimental procedure was approved by the Psychology Ethics committee and the Engineering health and safety department of Cardiff University.

2.2 Participant

A bald male (30 years of age) with no previous history of hearing problems participated in the measurements.

2.3 Laser Vibrometers

Data was collected via the Polytec™ PSV-500-3D system. This comprised of three scanning laser-Doppler vibrometer units. Each unit consists of a Class 2 He-Ne Laser with an output power of 1mW and an optical transducer that senses frequency shift of reflected light [19]. On the basis of the Doppler shift this is then used to determine the velocity and displacement of a point on an object. All three laser Doppler vibrometers were mounted on a tripod and were focused on the target in different planes (figure 1).

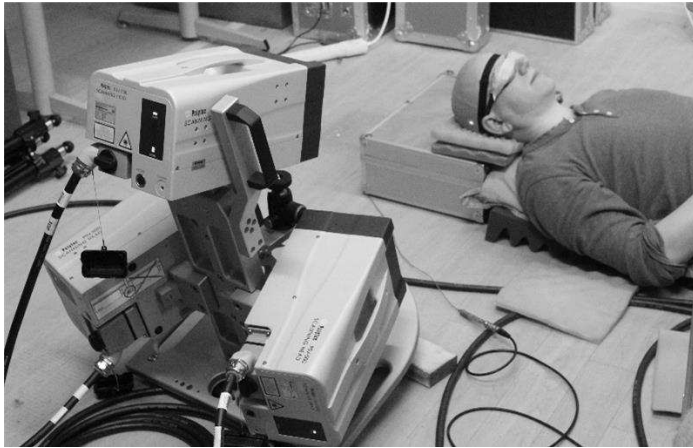


Figure 1 Three Polytec™ PSV-500 vibrometers focusing on participants right temporoparietal region (contralateral to the B71 bone transducer).

The simultaneous use of three laser Doppler vibrometers in different planes allowed the calculation of displacement and velocity in three orthogonal dimensions. The three lasers were focused on various reference points of interest before measurements were taken. This allowed a 3D reconstruction of the area of interest to be made.

2.4 Data collection

A B71 (RadioEar™) bone transducer was placed on the left temporal bone 55 mm behind the external auditory canal. This is the recommended surgical placement position for a bone-anchored hearing aid (Stenfelt et al. 2000). The participant wore laser-protective goggles at all times during testing. Laser measurements were made on the ipsilateral and contralateral temporoparietal region, occipital region and vertex. Testing was performed at four different frequencies (250, 500, 1000, 2000 Hz). All excitation frequencies were presented at one head position before the participant was repositioned to image a different region. The participant lay supine for all tests except for measurements of the occipital region for which he lay on his right side. For each test the orientation of the participant was altered so that all three lasers were able to have a clear line of sight on the area of interest. A single tone was played on the bone transducer by production of a sine wave with a sampling frequency of 44.1 kHz via Matlab™. Signals were sent to the B71 transducer via ESI Maya A44 audio interface and

to the Polytec PSV unit. The signal input was used by the Polytec PSV to synchronise the displacement and velocity to the phase cycle. Data collection at each viewing angle at each frequency was performed for 15 minutes with laser measurements performed at 2.56 MHz. In order to filter out noise and movement artefact from muscle movement, breathing and heartbeat only vibrations at the target frequency with a 2 Hz bandwidth were included.

2.5 Data Analysis

The 3D displacements relative to the phase of sound were reconstructed for each of the four areas of skull imaged. 3D reconstructions were initially generated perpendicular to the area imaged. In order to visualise displacement of all imaged areas along the axial plane, these images were rotated in 3D. The imaged occipital region was rotated 90 degrees towards the coronal plane. Both temporoparietal images were rotated towards the sagittal plane. The vertex image was not rotated as it was already imaged in the axial plane. Each of the four imaged areas were then merged and linked to the same phase cycle of one frequency in order to show displacement of the head as though looking down on the head from above. Reconstructions were performed at each of the four frequencies of excitation. Images of the displacement of the skull at each frequency were reconstructed every 10 degrees. Images were selected where displacement was at positive maximum (depicted in blue) and negative maximum (depicted in red) along the axial plane for each of the four imaged areas.

3. Results

Surface vibration of the skin in response to vibration of the underlying bone was detectable by our system at frequencies from 250 Hz (lowest tested) to 2 kHz. Figure 2 show the spatial pattern of displacement of the skin surface at various maxima for different frequencies. Animated sequences of each of the four frequencies imaged provide a much clearer impression of the movement, and can be viewed online.

Figure 2 (a) shows that at 250 Hz the left temporoparietal region (ipsilateral to the B71 bone transducer) is maximally positively displaced when the right is negatively displaced. 180 degrees later in the phase cycle the right temporoparietal region is maximally positively displaced and the left is negatively displaced, as shown in figure 2 (b).

Figure 2 (c) shows that at 500 Hz the left temporoparietal region is at maximal displacement when the right side is almost at maximal displacement. Similarly when the left side is negatively displaced the right side is almost at maximal negative displacement (as shown in figure 2 (d)). A surface wave displacement wave can also be visualised in the animation, travelling over the vertex of the skull as well as across the occipital region. During phase cycles when the temporoparietal regions are positively displaced the vertex and occipital regions are negatively displaced, and vice versa.

At 1000 Hz maximal positive and negative displacements are seen simultaneously at both temporoparietal regions (as shown in figure 2 (e) and (f)). During maximal positive displacement at the temporal region the occipital region and vertex are negatively displaced. Conversely during maximal negative displacement at the temporal region the vertex and occipital region are positively displaced.

The displacement pattern at 2000 Hz, shown in figure 2 (g-h), is less clear with no large displacement wave in the temporoparietal regions which were seen at all the lower frequencies. Instead, a complex

displacement wave is visualised in the animation, travelling across the vertex. No clear travelling wave is visible in the occipital region.

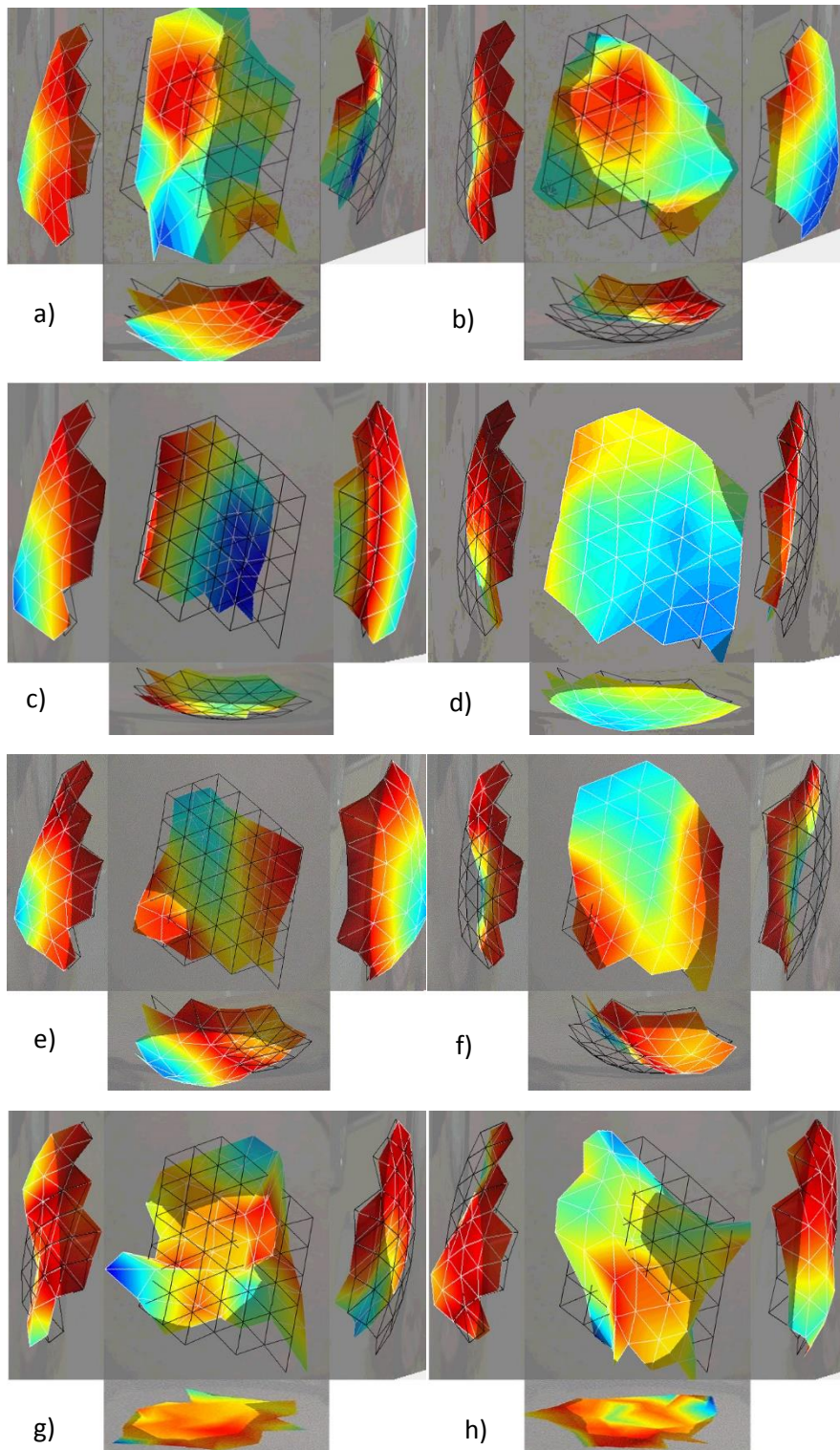


Figure 2 (a) showing relative transverse displacement at 250 Hz when the ipsilateral temporoparietal region is at maximum positive displacement and when the contralateral temporoparietal region is at maximal positive displacement (b). Relative displacement at 500 Hz when the ipsilateral temporoparietal region is at maximum positive displacement (c) and when the contralateral

temporoparietal region is at maximal negative displacement (d). Relative displacement at 1000 Hz when the ipsilateral temporoparietal region is at maximum positive displacement (e) and when the contralateral temporoparietal region is at maximal negative displacement (f). Relative displacement at 2000 Hz when the ipsilateral temporoparietal region is at maximum positive displacement (g) and when the contralateral temporoparietal region is at maximal negative displacement (h).

4. Discussion

4.1 Effects of frequency

Our measurements of skin displacements suggest that at 250 Hz the whole skull is moving from left to right, as shown in figure 3 (a). This finding is consistent with more direct measurements of the vibrational modes of the skull [20–22]. These studies found that the vibrational behaviour of the skull below frequencies of 400Hz is a rigid-body motion.

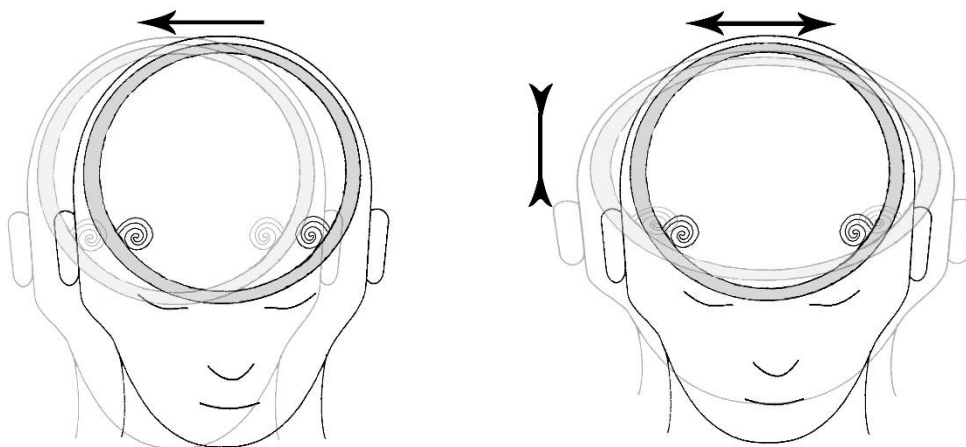


Figure 3 Visual representation of rigid-body motion (a) and mass-spring motion (b). Illustrations based on Stenfelt 2011.

At 500 Hz we found that large areas of the skull appeared to move into positive and negative displacement together. However, the displacements on both sides were not in unison. Previous studies using cadaver heads have concluded that at frequencies between 500 Hz and 1000 Hz the skull acts as a mass- spring system as shown in figure 3 (b). Our findings in a live participant seem to show a transition between rigid body motion and a mass-spring system at this frequency.

At 1000 Hz both temporoparietal regions move synchronously in positive and negative displacement. The vertex and occipital regions can be seen to be positively displaced when the temporoparietal regions are negatively displaced and vice versa. This again is consistent with findings from Stenfelt (2011) that the skull is acting as a mass-spring system at these frequencies.

Displacement findings at 2000 Hz are more difficult to interpret. There is no longer synchronisation between the displacements of the skull at different areas. However, there are visible transmission waves over the vertex. The displacement pattern over the temporoparietal regions and occipital regions are not so clear. However, these findings are consistent with previous research which found that between 1000 Hz and 2000 Hz the skull vibration transitioned from mass spring motion to wave transmission [21].

An alternative method of defining the vibrational modes which have been identified is via modal behaviour. This is particularly clear at 500 Hz, for which the skull vibration could be compared to the lowest vibrational mode of a sphere [23].

4.2 Limitations

We have shown that, using three vibrometers, it is possible to measure skin surface displacement at low frequencies (up to 2 kHz), that appears to reflect that of the underlying skull. At higher frequencies a clear pattern of wave transmission was not clear. This is likely related to the localised effect of the vibrational wave at high frequencies. It may be that there were not enough measurement points in order to have a high enough resolution to detect these signals. Future studies using this methodology should consider increasing the number of scanning points at higher frequencies. This will increase the time taken to collect data substantially.

One potential concern whilst performing this study was that our imaging would not detect skull movement but only movement of the skin and underlying soft tissues. Our measurements have assumed that the displacements detected were of the underlying skull as well as skin. It is possible

that this may be a confounding factor when assessing the movement of the skull, as these displacements could be due to pressure waves over the soft tissues of the skull rather than the bony skull itself. However, consistency with the literature leads us to believe that our findings at frequencies between 250 Hz and 1000 Hz are unlikely to be due to anything other than the movement of the underlying skull in rigid body motion or a mass spring like behaviour. Additionally, we found that at frequencies of 250 Hz displacement at the vertex was in the region of 140 nm. At the occiput maximal displacement was up to 6 nm, whilst contralateral displacement was 32 nm. We therefore feel it is unlikely that our measurements are due to soft tissue vibration travelling over the skull as smaller displacements were detected closer to the bone transducer.

However, our findings of wave transmission at 2000 Hz could be explained by pressure wave transmission in the skin and soft tissue alone. Nonetheless, all our findings support previous research, which has found the same vibrational modes in dry skulls at similar frequencies.

Another potential concern is that the participant's head was resting against a rigid object. This in itself could change the vibrational characteristics of the head. However, if the participant was allowed to sit up, movement from the participant would have likely made data collection impossible as well as introducing a new confounding factor such as increased tension from the muscles attaching to the occipital region of the head.

4.3 Potential Applications

This new methodology opens up potential research areas for sound transmission pathways in individuals who receive a high proportion of bone-conducted sound, such as divers, individuals wearing hearing protection, as well as those with conductive hearing losses.

There are potential research opportunities for developing bone-conducted-sound cancellation techniques whereby bone-conducted sound and its phase can be monitored in real time and cancelled via a bone transducer via a feedback mechanism. This could be key in overcoming the bone conduction

limit, at which hearing protection devices cease to be effective. This limit exists due to the vibration of the skull causing a very high level of bone-conducted sound to be transferred. It is a particular problem on aircraft carrier flight decks.

Future research using a similar technique could present broadband noise to the bone transducer and image different areas of the skull. Scanning LDV has the ability to extract the differing modes of vibration at each frequency. This allows the potential to visualise areas of the temporal bone where there are clear anti-resonance frequencies. Pure tones at those frequencies can then be presented to see if they result in strong lateralisation to the opposite ear. This could allow a clearer understanding of the relative importance of anti-resonance frequencies of the skull compared to that of the ossicles in lateralisation.

LDV also allows the potential to investigate how two bone transducers on each mastoid affect the movement of the skull at difference frequencies. This could allow calibration of a cross talk cancellation system whereby sound from one bone transducer is cancelled at the contralateral cochlea by a contralateral bone transducer[24,25].

5. Conclusion

We have shown that LDV applied to the scalp is a viable method for measuring displacement of the underlying skull when stimulated by a bone transducer. Our findings in a live participant correspond well with previous research on dry skulls and cadaver heads [10]. 3D reconstructions demonstrated rigid body motion of the skull at 250 Hz and a transition to a mass spring system between 250-500 Hz. At frequencies of 1000 Hz we showed clear evidence of a mass-spring effect. However, the number of points used for each scan did not allow high enough resolution to identify clear evidence of a wave transmission at 2000 Hz via localised compression of parts of the skull.

This methodology allows further research into methods of utilising two BAHAs in a cross-talk cancellation system. This could be achieved by measuring cranial displacements over the temporal

bones using LDV at differing frequencies, and would allow one BAHA to be calibrated in order to cancel the vibrations detected from the LDV by the other BAHA.

6. Acknowledgement

This research is sponsored by Cochlear Bone Anchored Solutions AB.

7. References

- [1] Håkansson B, Carlsson P, Tjellström a. The mechanical point impedance of the human head, with and without skin penetration. *J Acoust Soc Am* 1986;80:1065–75.
- [2] Wismer MG, O’Brien WD. Evaluation of the vibrational modes of the human skull as it relates to bone-conducted sound. *J Acoust Soc Am* 2010;128:2792–7. doi:10.1121/1.3493432.
- [3] Rowan D, Gray M. Lateralization of high-frequency pure tones with interaural phase difference and bone conduction. *Int J Audiol* 2008;47:404–11. doi:10.1080/14992020802006055.
- [4] Stenfelt S, Wild T, Hato N, Goode RL. Factors contributing to bone conduction: The outer ear. *J Acoust Soc Am* 2003;113:902. doi:10.1121/1.1534606.
- [5] Tonndorf J, Khanna SM. Displacement pattern of the basilar membrane: a comparison of experimental data. *Science* 1968;160:1139–40.
- [6] Zwislocki JJ. Middle ear, cochlea, and Tonndorf. *Am J Otolaryngol* 1981;2:240–50.
- [7] Berger EH, Kieper RW, Gauger D. Hearing protection: Surpassing the limits to attenuation imposed by the bone-conduction pathways. *J Acoust Soc Am* 2003;114:1955. doi:10.1121/1.1605415.
- [8] Guignard J, Stieger C, Kompis M, Caversaccio M, Arnold A. Bone conduction in Thiel-embalmed cadaver heads. *Hear Res* 2013;306:115–22. doi:10.1016/j.heares.2013.10.002.
- [9] Homma K, Shimizu Y, Kim N, Du Y, Puria S. Effects of ear-canal pressurization on middle-ear bone- and air-conduction responses. *Hear Res* 2010;263:204–15. doi:10.1016/j.heares.2009.11.013.
- [10] Stenfelt S, Håkansson B, Tjellström a. Vibration characteristics of bone conducted sound in vitro. *J Acoust Soc Am* 2000;107:422–31. doi:10.1121/1.428314.
- [11] Håkansson B, Brandt A, Carlsson P, Tjellstrom A. Resonance frequencies of the human skull in vivo. *Acoust Soc Am* 1993;95:1474–81.
- [12] Khalil TB, Viano DC, Smith DL. Experimental analysis of the vibrational characteristics of the human skull. *J Sound Vib* 1979;63:351–76. doi:10.1016/0022-460X(79)90679-5.
- [13] Voss SE, Rosowski JJ, Merchant SN, Peake WT. Acoustic responses of the human middle ear. *Hear Res* 2000;150:43–69.
- [14] Stenfelt S, Hato N, Goode RL. Round window membrane motion with air conduction and bone conduction stimulation. *Hear Res* 2004;198:10–24. doi:10.1016/j.heares.2004.07.008.
- [15] Homma K, Du Y, Shimizu Y, Puria S. Ossicular resonance modes of the human middle ear for

- bone and air conduction. *J Acoust Soc Am* 2009;125:968–79. doi:10.1121/1.3056564.
- [16] Eeg-Olofsson M, Stenfelt S, Tjellström A, Granström G. Transmission of bone-conducted sound in the human skull measured by cochlear vibrations. *Int J Audiol* 2008;47:761–9. doi:10.1080/14992020802311216.
- [17] McKnight CL, Doman D a, Brown J a, Bance M, Adamson RB a. Direct measurement of the wavelength of sound waves in the human skull. *J Acoust Soc Am* 2013;133:136–45. doi:10.1121/1.4768801.
- [18] Kitamura T. Measurement of vibration velocity pattern of facial surface during phonation using scanning vibrometer. *Acoust Sci Technol* 2012;33:126–8. doi:10.1250/ast.33.126.
- [19] Rohrbaugh JW, Polytec GmbH. *Measuring and Scanning Physiological Signals*. 2010.
- [20] Stenfelt S, Goode RL. Transmission properties of bone conducted sound: Measurements in cadaver heads. *J Acoust Soc Am* 2005;118:2373. doi:10.1121/1.2005847.
- [21] Stenfelt S. Acoustic and physiologic aspects of bone conduction hearing. *Adv Otorhinolaryngol* 2011;71:10–21.
- [22] von Békésy G. *Experiments in Hearing*. vol. 88. New York, NY: McGraw-Hill; 1960. doi:10.1121/1.399656.
- [23] Russell D a. Basketballs as spherical acoustic cavities. *Am J Phys* 2010;78:549. doi:10.1119/1.3290176.
- [24] Liao C. Application of cross-talk cancellation to the improvement of binaural directional properties for individuals using bone anchored hearing aids (BAHA). 2010.
- [25] Mcleod RWJ, Culling JF. Measurements of inter-cochlear level and phase differences of bone-conducted sound. *J Acoust Soc Am* 2017;141:3421–9. doi:10.1121/1.4983471.